Towards a Tetravalent Chemistry of Colloids

David R. Nelson

Lyman Laboratory of Physics, Harvard University, Cambridge, MA 02138

(February 1, 2008)

Abstract

We propose coating spherical particles or droplets with anisotropic nano-sized objects to allow micron-scale colloids to link or functionalize with a four-fold valence, similar to the sp^3 hybridized chemical bonds associated with, e.g., carbon, silicon and germanium. Candidates for such coatings include triblock copolymers, gemini lipids, metallic or semiconducting nanorods and conventional liquid crystal compounds. We estimate the size of the relevant nematic Frank constants, discuss how to obtain other valences and analyze the thermal distortions of ground state configurations of defects on the sphere.

Self-assembly or functionalization of micron-sized particles has many potential uses, including particle-based bioassays [1], catalysis [2] and photonic band gap materials [3]. However, attaching a small, predetermined number of chemical groups, DNA strands or kinesin molecules to considerably larger colloidal spheres can be an inefficient process, since the number of ligands per sphere is highly variable. If the ligand concentration in solution is kept very low, many spheres will have no ligands at all. Higher ligand concentrations require tedious sorting methods such as gel electrophoresis to select the spheres with the correct number of attached objects [4].

Controlled fabrication of *tetravalent* colloids would be of particular interest. Dense glassy and crystalline colloidal arrays (possibly involving DNA linker elements [5]) usually display

the large number of near neighbors ($Z = 12-14$) characteristic of an isotropic pair potential [6]. We analyze here a means by which micron-scale colloids could link or be functionalized with, say, a *four*-fold valence, similar to the sp^3 hybridized chemical bonds on an Angstrom scale associated with, e.g., carbon, silicon and germanium. We suggest in particular coating spherical colloid particles (or polymerizable liquid droplets) with anisotropic objects such as metallic or semiconducting nanorods, gemini lipids, triblock copolymers or conventional nematogens. If the particles are sufficiently anisotropic, a two-dimensional nematic liquid crystal phase will appear on the surface. The spherical topology then forces four strongly repulsive disclination defects into the ground state, a circumstance which would allow creation of novel tetravalent colloidal materials with chemical linkers or DNA strands anchored at the defect cores. In contrast to fcc and bcc colloid arrays, a tetravalent colloidal crystal with a diamond lattice structure and appropriate dielectric contrast is predicted to have a very large photonic band gap [7]. More generally, colloidal particles with a 1-, 2-, 3- or 4-fold valence would also allow creation of functionalized micron-sized objects similar to the molecules characteristic of organic chemistry, and could be useful for bioassays and catalysis.

A two-dimensional nematic at a *flat* interface is described by a Frank elastic free energy, namely [8]

$$F = \frac{1}{2}\int d^2r[K_1(\vec{\nabla}\cdot\vec{n})^2 + K_3(\vec{\nabla}\times\vec{n})^2] \tag{1}$$

where $\vec{n}(\mathbf{r})$ is a slowly varying director field describing the local molecular alignment and K_1 and K_3 are, respectively, splay and bend elastic constants. (The twist elastic constant K_2 is absent in two dimensions.) The effect of thermal fluctuations (which are very strong in $d = 2$) in a sufficiently large system is to renormalize these elastic constants to a single common value K [9]. As a first approximation, we can take $K \approx \sqrt{(K_1K_2)}$. The nature of point-like defects in nematic textures depends sensitively on the symmetry of the constituent particles. For tilted molecules (as might be the case in freestanding smectic liquid crystal layers [10] or Langmuir-Blodgett films [11]), the order parameter is a vector representing the projection of the molecules onto the plane. The 2π rotational symmetry leads to defects like

the vortex shown in Fig. 1a. An unbinding of vortex-antivortex pairs causes a transition out of the ordered state whenever $K < 2k_BT/\pi$ [12]. In contrast, the order parameter for molecules which lie down completely on a liquid or solid interface has the higher symmetry of a *headless* arrow. The symmetry under rotations by π which results would apply to nematically ordered monolayer phases of, e.g., gemini lipids [13], ABA triblock copolymers [14] and nanorods made of gold [15], $BaCrO_4$ [16] or CdSe [17]. In this case, it is well known [8,18] that the vortex in Fig. 1a is unstable to the two disclinations shown in Fig. 1b. The 180 degree rotational symmetry allows these mutually repelling defects to separate—these defects would be bound with a linear potential for an order parameter with a *vector* symmetry. Disclination unbinding leads to a transition at a temperature which is four times smaller, i.e., for $K < k_BT/2\pi$.

FIGURES

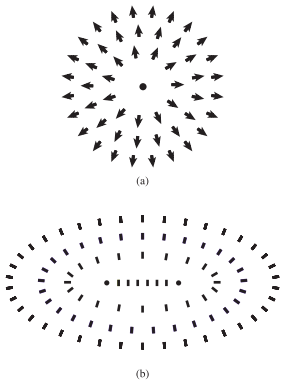

FIG. 1. (a) Vortex configuration of a *vector* order parameter in the plane. The order parameter rotates by 2π on a circuit around the defect at the center. (b) The texture in (a) is unstable to two disclinations for a configuration of headless vectors in the plane. The order parameter rotates by π on a circuit around each of the defects marked by small dots.

Although pairing of defects and antidefects leads to a virtually defect-free equilibrium state at high densities or low temperatures at flat interfaces, the situation is quite different on surfaces with a nonzero Gaussian curvature. For liquid crystal phases embedded in an arbitrary curved surface, the free energy in the one Frank constant approximation reads

$$F = \frac{1}{2} K \int d^2x \sqrt{g(x)} [\partial_i n^j + \Gamma^j_{ki} n^k]^2, \tag{2}$$

where $x = (x_1, x_2)$ represents a set of internal coordinates, the director is $\vec{n} = \vec{n}(x_1, x_2)$, g is the determinant of the metric tensor $g_{ij}(x)$, and the $\{\Gamma^j_{ki}\}$ are connection coefficients associated with parallel transport of the order parameter. For a rigid sphere of radius R with polar coordinates (θ, ϕ), we have $\sqrt{g} = R^2 \sin\theta$, $\Gamma^\theta_{\phi\phi} = -\sin\theta\cos\theta$, $\Gamma^\phi_{\theta\phi} = \Gamma^\phi_{\phi\theta} = \cot\theta$ and all other $\Gamma^j_{ki} = 0$. The free energy (2) also describes hexatic liquids (i.e., liquid crystals with a *six*-fold symmetry) on curved surfaces [19,20]. In this case, the Gaussian curvature of the sphere produces an unpairable excess of 12 "disclinations" (i.e., defects around which the order parameter rotates by $2\pi/6 = 60$ degrees) at the vertices of an icosahedron in the ground state [19]. In an elegant paper, Lubensky and Prost have studied the ground states of more general order parameters with a p-fold symmetry on the sphere [21]. In this

case, the order parameter rotates by $2\pi/p$ on a circuit which encloses the minimum energy defect, and the j-th defect is characterized by an integer $n_j = \pm 1, \pm 2, \cdots$, which specifies the winding angle $2\pi n_j/p$. The Poincaré index theorem [22] then implies that

$$\sum_j n_j = 2p, \tag{3}$$

for any ordered texture embedded in a surface with the topology of sphere. With our conventions, positive winding numbers are favored by positive Gaussian curvature and negative winding numbers are favored by saddle-like regions of negative Gaussian curvature.

As pointed out by Lubensky and Prost, the ground state of a two-dimensional nematic texture on a sphere consists of four $n_j = +1$ disclinations at the vertices of a tetrahedron [21]. Aligned states of *vector* order parameters on the sphere, on the other hand, will be interrupted by just *two* $n_j = +1$ vortices, corresponding to the familiar north and south pole singularities of the lines of latitude and longitude of spherical cartography. *Splay* dominated textures for vector and headless vector order parameters on the sphere are illustrated in Figs. 2(a) and 2(b), respectively [23]. The texture in Fig. 2(a) can in fact be transformed into those of Fig. 2(b) by invoking the instability shown in Fig. 1. The inevitable defects associated with liquid crystalline textures on the sphere could be exploited to create colloids with a 2- and 4-fold valence in a number of ways. If, say, gold is deposited on coated solid spheres, the texture will act as mask such that the two or four "bald spots" at the defect cores will be coated preferentially. One could then attach, e.g., thiol chemical linkers via the extra gold at the bald spots. Alternatively, one could introduce DNA linkers attached to amphiphillic molecules on polymerizable liquid drops. Linkers immiscible with the aligned liquid crystalline molecules will segregate preferentially at the defect cores, similar to impurity segregation at grain boundaries in conventional metallurgy. While we do not wish to minimize the experimental challenges, the examples cited above illustrate the possibilities for directional bonding associated with ordered states in spheres. *Topology* can be used to create a micron-scale directional chemical bonds similar to those produced by quantum mechanics on an Angstrom scale.

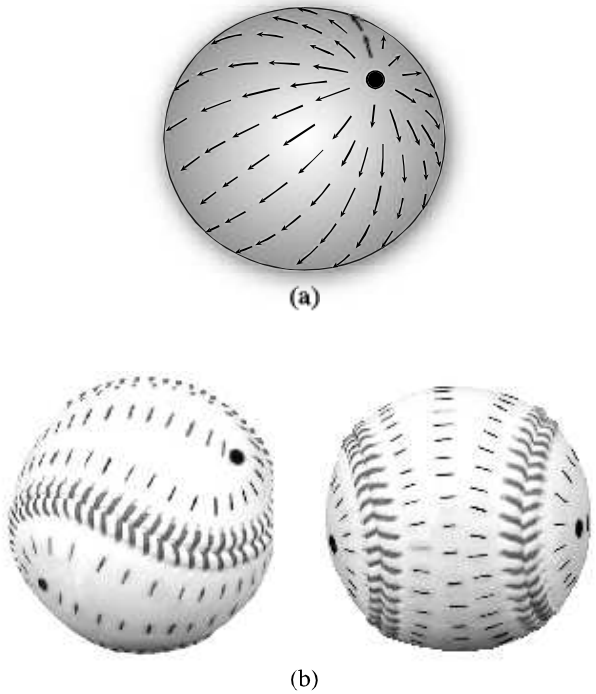

FIG. 2. (a) Splay vector order parameter configuration on a sphere. There are +1 vortices at the north and south pole. (b) Two views of a splay configuration of headless vectors on the sphere. There are four disclinations at the vertices of a tetrahedron. (Note that one row of nematogens tracks the seam of a baseball!)

To explore the fidelity of directional bonds created by the above scheme, we need a more detailed analysis of ground states on the sphere and their stability to thermal fluctuations. To this end, we exploit an alternative representation of Eq. (2) in terms of a defect density

$$s(x) = \frac{2\pi}{p} \sum_j n_j \delta^{(2)}(x - x_j)/\sqrt{g(x_j)} \tag{4}$$

and the Gaussian curvature $G(x)$ namely [24]

$$F = \frac{1}{2} K \int d^2x \sqrt{g(x)} \int d^2y \sqrt{g(y)} [G(x) - s(x)] \frac{1}{\Delta}\Big|_{x,y} [G(y) - S(y)]. \tag{5}$$

Here, $1/\Delta$ denotes the inverse of Laplacian operator,

$$\nabla^2 \equiv \frac{1}{\sqrt{g}} \sum_j \partial_i (\sqrt{g} g^{ij} \partial_j), \tag{6}$$

appropriate to a curved surface with metric $g_{ij}(x)$ and the defects sit at positions $\{x_j\}$ with a set of integer winding numbers $\{n_j\}$. The resulting energy for liquid crystal textures with a p-fold symmetry on the sphere is quite simple,

$$F = -\frac{\pi K}{2p^2} \sum_{i \neq j} n_i n_j \ln(1 - \cos \beta_{ij}) + E(R) \sum_j n_j^2. \tag{7}$$

Here the angle $\beta_{ij} = d_{ij}/R$, where d_{ij} is the geodesic distance between defects i and j, and $E(R)$ is a defect self-energy,

$$E(R) = \frac{\pi K}{p^2} \ln(R/a) + E_c. \tag{8}$$

The quantity E_c is a microscopic energy which depends on the details of the particle interactions near the defect core on length scales of order a, where a is the particle separation.

The repulsive interaction between defects in (7) is very long-range, extending out to a significant fraction of the circumference of the sphere. Unlike conventional Coulomb interactions between charged particles, this interaction cannot be screened if the order on the surface is strong. The defect self-energy (8) diverges logarithmically with the sphere radius and accounts for the instability indicated in Fig. 1. To see this, note that the 2π vortex of Fig. 1a in a medium of aligned headless vectors corresponds to a topological charge $n = 2$ with $p = 2$. Two such defects at the north and south poles contribute a logarithmically diverging term in the energy, $2[(n/p)^2 \pi K \ln(R/a)] = 2\pi K \ln(R/a)$. If, however, each defect splits into two disclinations with charge $n = 1$, the corresponding contribution is $4[(n/p)^2 \pi K \ln(R/a)] = \pi K \ln(R/a)$. We see that the dominant term in the energy for large R/a has been reduced by a factor of two. It is easy to check that the ground state energy configuration with the repulsive interaction in (7) is indeed two vortices at the north and south poles, and four disclinations at the vertices of a tetrahedron for vector and nematic ordering, respectively.

The long-range interaction in Eq. (7) will resist thermal disruption of the ordered defect arrays mentioned above. To investigate this effect for vector order parameters, we define a bending angle θ between the two antipodal defects by setting $\beta_{ij} = \pi + \theta$. Upon expanding (7) in θ, we find that $F \approx \text{const.} + (\pi/4) K \theta^2$. The equipartition theorem now shows that for valence $Z = 2$ colloids in the limit $K >> k_B T$,

$$\langle \cos \beta_i \rangle \approx -1 + \frac{1}{2} \langle \theta^2 \rangle$$

$$\approx -1 + \frac{k_B T}{\pi K} \qquad (Z = 2). \tag{9}$$

Determining the thermal disruption of the tetrahedral ground state which results for nematic order on a sphere is more involved. To get a rough estimate, imagine freezing three of the disclinations (with $j = 1 - 3$) at the vertices of a tetrahedron and then allow the remaining defect (with $j = 0$) to fluctuate away from its equilibrium position on the z axis. Upon expanding Eq. (7) in the polar coordinates (θ, ϕ) of this defect about an equilibrium configuration with tetrahedral angles $\beta_{ij} = \cos^{-1}(-1/3)(i \neq j)$, we obtain $F \approx$ const. $+ (3\pi/16)K\theta^2$, which leads to $\langle \theta^2 \rangle = 8k_B T/3\pi K$. A more precise analysis follows from rewriting Eq. (7) (with $p = 2$ and all $n_j = 1$) as

$$F = -\frac{\pi K}{8} \sum_{i \neq j} \ln(1 - \mathbf{m}_i \cdot \mathbf{m}_j) + 4E(R), \tag{10}$$

where the $\mathbf{m}_j$ are three-dimensional unit vectors specifying the positions of the defects on the sphere. Upon writing $\mathbf{m}_j = \mathbf{m}_j^0 + \delta \mathbf{m}_j$, where $\delta \mathbf{m}_j \perp \mathbf{m}_j^0$ represents a small deviation from a perfect tetrahedral configuration such that $\mathbf{m}_i^0 \cdot \mathbf{m}_j^0 = -1/3$ $(i \neq j)$, the energy to quadratic order is

$$F = \text{const.} + \frac{\pi K}{4} \sum_{i,j} \sum_{\alpha\beta} M_{ij}^{\alpha\beta} \delta m_i^\alpha \delta m_j^\beta, \tag{11}$$

where α and β run over the two independent components of the $\{\delta \mathbf{m}_j\}$ and $M_{ij}^{\alpha\beta}$ is an 8×8 matrix describing the deformations of a perfect tetrahedron on the sphere. The eigenvalues of this matrix can be classified according to the irreducible representations of the symmetry group of the tetrahedron, similar to the analysis of the vibrational modes of the methane molecule [25]. A somewhat lengthy calculation shows that the eigenvalue spectrum of $M_{ij}^{\alpha\beta}$ reads

$$\{\lambda_j\} = (3/8)\{0, 0, 0, 1, 1, 2, 2, 2\}. \tag{12}$$

Rigid body rotations generate the three normal modes with zero eigenvalues. The remaining eigenvectors generate two- and three-dimensional representations of the tetrahedral symmetry group. The doublet corresponds to a shear-like twisting deformation of the tetrahedron

while the non-zero triplet of eigenvalues represents stretching or compression of vectors joining neighboring defects. Upon re-expressing the free energy (11) in terms of the normal modes we calculate that the deviation for valence $Z = 4$ colloids from perfect tetrahedral angles due to thermal fluctuations is given by

$$\langle \cos \beta_{ij} \rangle \approx -\frac{1}{3} + \frac{16}{9\pi} \frac{k_B T}{K} \qquad (Z = 4). \tag{13}$$

Because the distortion from perfect alignment for $Z = 2$ and $Z = 4$ colloids is proportional to $k_B T/K$, it is of some interest to determine this quantity for a nematic phase formed, say, from anisotropic rods [15–17]. Close to the nematic ordering transition, we expect the universal values [9, 12] $K_1 = K_3 = K = 2k_B T/p^2\pi$, suggesting fairly large fluctuations in the bond angles associated with the topology-induced directional bonding for $p = 1$ ($Z = 2$) and $p = 2$ ($Z = 4$). However, these angles are more robust to thermal fluctuations in the high density limit where $K >> k_B T$. Suppose the rods have length ℓ and diameter d. Estimates are conveniently constructed by adapting results from an Onsager theory for the *bulk* Frank constants $K_1^{(3)}$ and $K_3^{(3)}$ in three dimensions, a theory valid in the limit $\ell >> d$ [26]. For a monolayer film of thickness d, we have $K_i \approx dK_i^{(3)}$. For well developed nematic order, the numerical results of Lee and Meyer [26] when applied to thin films of thickness d lead to the approximate formula

$$K \approx \sqrt{K_1 K_3} \approx 0.10 \rho^2 \ell^4 k_B T, \tag{14}$$

where ρ is the *areal* density of nematogens. This density is of order $\rho \sim 1/\ell^2$ at the ordering transition but rises to $\rho \sim 1/\ell d$ deep inside the nematic phase. Thus, in the dense limit $K = 0.10\ (\ell/d)^2 k_B T$, so that $k_B T/K \approx 10\ (d/\ell)^2$. We see that the bond angle fluctuations become quite small for large ℓ/d, which is of order 10 in the experiments of Ref. 17.

The Onsager theory calculations of Ref. [26] show that the bend elastic constant K_3 can be much larger than the splay constant K_1 for highly anisotropic hard rods. This asymmetry favors the "lines of longitude"' texture of Fig. 2a over a texture which follows the lines of latitude. These two configurations are degenerate in the one Frank constant approximation.

A latitudinal texture would dominate if $K_3 << K_1$. The nematic texture which replaces Fig. 2b in this limit is shown schematically in Fig. 3, together with possible polymer linking elements emerging from defects at the vertices of a tetrahedron. Investigations of these textures for arbitrary K_1/K_3 are currently in progress using a lattice model of a nematic [27]. Direct simulations of two-dimensional hard rod fluids [28] on a sphere would also be of interest, as would investigations of two-dimensional smectic order on a sphere [27].

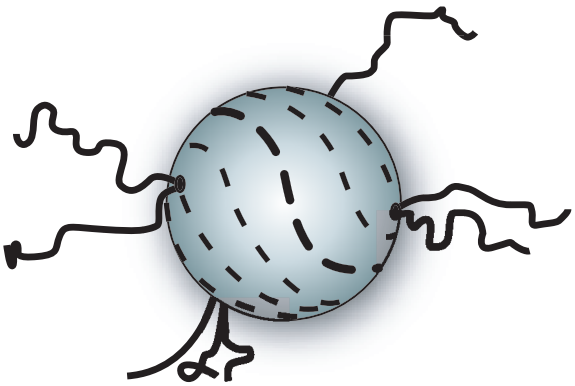

FIG. 3. Bend texture of headless vectors on the sphere appropriate to $K_1 > K_3$. The preferred configuration for $K_1 < K_3$ is the splay texture shown in Fig. (2b). Polymer linkers are shown schematically emerging from the tetrahedron of four disclinations.

We have argued that coating of colloidal particles with vector or nematic degrees of freedom could be used to construct micron-sized objects with valence $Z = 2$ or $Z = 4$. Other valences and mechanisms are also possible. For example, the *bulk* nematic liquid crystal droplets which appear in polymer dispersed liquid crystals typically have two surface defects [29], which might also lead to particles with functionality $Z = 2$. Biaxial nematic droplets should have a single "boojum" defect on their surface [18], which upon polymerization might lead to a $Z = 1$ micron-sized analogue of the hydrogen atom. Finally, tetravalent colloids with, say, DNA linkers could be tethered via one of the four defects to a surface (see Fig. 4). This configuration could be useful for colloid-mediated catalysis [2], and the remaining crosslinks in the plane of the surface would have a 3-fold valence, i.e. a colloidal analogue of sp^2 hybridization.

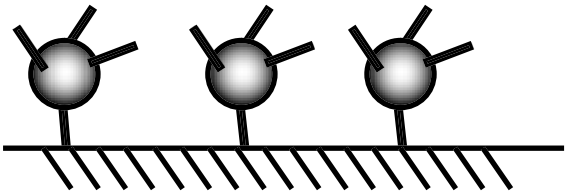

FIG. 4. Tetravalent colloids tethered to a planar substrate. The remaining linkers can connect with a 3-fold valence $Z = 3$.

ACKNOWLEDGMENTS

It is a pleasure to acknowledge helpful discussions with P. Alivisatos, S. Block, W. Dressick, F. Dyson, G. Joyce, M. Kilfoil, R.B. Meyer, C. Mirkin, W. Press, V. Vitelli and P. Wiltzius. This work was supported by the NSF through the Harvard MRSEC via Grant No. DMR98–09363 and through Grant No. DMR97–14725.

REFERENCES

[1] See, e.g., K. Svoboda, C.F. Schmidt, B.J. Schnapp, and S.M. Block. Nature **365**, 721 (1993).

[2] S.L. Brandow, M.S. Chen, T. Wang, C.S. Duleey, J.M. Calvert, J.F. Bohland, G.S. Calabrese, and W.J. Dressick. J. Electrochem. Soc. **144**, 3426 (1997).

[3] J. Joannopoulos. Nature **414**, 257 (2001); see also "Challenges and Opportunities at the Interface of Biology and Nanotechnology," JASON Presentation JSR01-110.

[4] D. Zanchet, C.M. Micheel, W.J. Parak, D. Gerion, and A.P. Alivisatos. Nanoletters **1**, 32–35 (2001).

[5] C.A. Mirkin, R.L. Letsinger, R.C. Mucic, and J.J. Storhoff. Nature **382**, 607–609 (1996).

[6] U. Gasser, E. R. Weeks, A. Schofield, P.N. Pusey, and D.A. Weitz. Science **292**, 258 (2001).

[7] K.M. Ho, C.T. Chang, and C.M. Soukoulis. Phys. Rev. Lett. **65**, 3152 (1990).

[8] P.G. deGennes and J. Prost. The Physics of Liquid Crystals (Oxford University Press, Oxford, 1993).

[9] D.R. Nelson and R.A. Pelcovits. Phys. Rev. **B16**, 2191 (1977).

[10] C.C. Huang. In *Bond-Orientational Order in Condensed Matter Systems*, edited by K. Standburg (Springer, Berlin, 1992).

[11] C. Knobler and R. Desai, Ann. Rev. Phys. Chem. **43**, 207 (1992).

[12] D.R. Nelson and J.M. Kosterlitz. Phys. Rev. Lett. **39**, 1201 (1977).

[13] F.M. Menger and C.A. Littau, J. Am. Chem. Soc. **115**, 10,083–10,090 (1993).

[14] See, e.g., M.W. Matsen and M. Schick. Macromolecules **27**, 187 (1990).

[15] B. Nikoobakht, Z.L. Wang and M.A. El-Sayed, J. Phys. Chem. B **104**, 8635–8640 (2000).

[16] F. Kim, S. Kwan, J. Akana, and P. Yang, J. Am. Chem. Soc. **123**, 4360–4361 (2001).

[17] L. Li, L. Manna, J. Hu, and A.P. Alivisatos, "Quantum Rod Liquid Crystals," (Nanoletters, in press).

[18] N.D. Mermin, Rev. Mod. Phys. **51**, 591 (1979).

[19] D.R. Nelson. Phys. Rev. **B28**, 5515 (1983).

[20] D.R. Nelson and L. Peliti. J. de Physique **48**, 1085 (1987).

[21] T.C. Lubensky and J. Prost, J. Phys. II (France) **2**, 371 (1992).

[22] See, e.g., M. Spivak, *A Comprehensive Introduction to Differential Geometry* (Publish or Perish, Berkeley, 1979).

[23] We shall argue below that *bend* dominated textures are likely to have a higher energy.

[24] M. Bowick, A. Travesset, and D.R. Nelson, Phys. Rev. **B62**, 8738 (2000). See also S. Sachdev and D.R. Nelson, J. Phys. **C17**, 5473 (1984) and Ref. [21].

[25] E.B. Wilson, Jr., J.C. Decius and P.C. Cross. *Molecular Vibrations: The Theory of Infrared and Raman Vibrational Spectra* (Dover, New York 1980).

[26] S.-D. Lee and R.B. Meyer. J. Chem. Phys. **84**, 3443–3448 (1986); See also J.P. Straley, Phys. Rev. **A8**, 2181 (1973), and A. Poniewierski and J. Stecki, Molecular Physics **38**, 1931 (1979).

[27] , V. Vitelli and D.R. Nelson, to be published.

[28] M.A. Bates and D. Frenkel. J. Chem. Phys. **112**, 10034 (2000).

[29] See, e.g., P. Mach, R. Nortrup, J.A. Rogers and P. Wiltzius, Appl. Phys. Lett **78**, 3592 (2001).

FIGURES

FIG. 1. (a) Vortex configuration of a *vector* order parameter in the plane. The order parameter rotates by 2π on a circuit around the defect at the center. (b) The texture in (a) is unstable to two disclinations for a configuration of headless vectors in the plane. The order parameter rotates by π on a circuit around each of the defects marked by small dots.

FIG. 2. (a) Splay vector order parameter configuration on a sphere. There are +1 vortices at the north and south pole. (b) Two views of a splay configuration of headless vectors on the sphere. There are four disclinations at the vertices of a tetrahedron. (Note that one row of nematogens tracks the seam of a baseball!

FIG. 3. Bend texture of headless vectors on the sphere appropriate to $K_1 > K_3$. The preferred configuration for $K_1 < K_3$ is the splay texture shown in Fig. (2b). Polymer linkers are shown schematically emerging from the tetrahedron of four disclinations.

FIG. 4. Tetravalent colloids tethered to a planar substrate. The remaining linkers can connect with a 3-fold valence $Z = 3$.